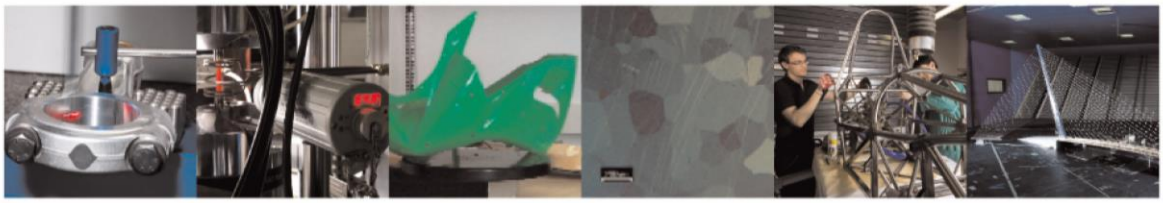

# Coupled Eulerian-Lagrangian technique for microcutting FE-modelling of AISI1045 steel

Afsharhanaei, Ali; Parenti, Paolo; Annoni, Massimiliano

This is a post-peer-review, pre-copyedit version of an article published in International Journal of Machining and Machinability of Materials (IJMMM), Vol. 21, No. 3, 2019. The final authenticated version is available online at: http://dx.doi.org/10.1504/IJMMM.2019.099484



**Section B: Revised Manuscript**

# Coupled Eulerian-Lagrangian technique for microcutting FE-modelling of AISI1045 steel


## Abstract

Deepen the analysis of the cutting process mechanics beneath the tool edge radius is one of the primary concerns in micro cutting. This paper shows that Coupled Eulerian Lagrangian (CEL) technique applied to micro machining process modelling can be a valid alternative comparison to traditional chip formation modeling methods, as the Arbitrary Lagrangian Eulerian (ALE) and Continuous Remeshing of Lagrangian domain (CRL). CEL does not require separation criteria since it implements workpiece modeling by means of Eulerian domain — whilst keeping tool in Lagrangian domain — by avoiding mesh topography changes. This work fills the gap that exists in literature about the application of CEL technique in micro cutting modeling. The developed 3D CEL entails a full set of thermo-mechanical input parameters and is validated by conducting micro orthogonal cutting experiments. A specifically equipped ultra-high precision machining center is used for cutting AISI1045 at different cutting speeds and uncut chip thicknesses — varied respectively up to 300 m/min and 60 µm. CEL approach resulted capable to predict the process outputs, i.e. namely chip thickness and cutting/thrust forces, within a mean error of around 20%, comparable to existing techniques and showed better accuracy in actual chip thickness prediction. Tool tip temperature and contact pressure investigations have been based on simulations, underlining the significant role played by cutting speed on both outputs especially when tool edge geometry dominates into the cutting, whilst confirming a minor role of the uncut chip thickness. Finally, direct comparison with ALE approach confirmed that CEL shows similar computational efficiency its final implementation in micro cutting modelling.

**Keywords:** Finite Element Method, Micro cutting, Coupled Eulerian Lagrangian, Cutting Forces, Chip Thickness, Tool Tip Temperature

# 1. Introduction

## 1.1. Finite Element Modeling in machining process

A deeper understanding of mechanics involved in chip formation of micro and macro cutting processes is fundamental for improving cutting action by proper tool design and cutting process setups. On one side, thermal analysis, consisting in understanding sources and amount of heat generation in the process, can help technologists to design process parameters to minimize heat generation on contact zone, preventing tool wear and consequently reducing machining costs. On the other side, prior knowledge about cutting forces allows to better understand the required stiffness of machine tool fixtures for each specific cutting condition. However, studying these quantities with traditional techniques is expensive and difficult. For example, small contact areas between tool and chip makes temperature distribution measure and other fundamental process variables such as contact pressure distribution very challenging. This issue is particularly pronounced in micro scale cutting, where in general the amount of material removed is extremely small [1]and where the contact length can be less than 200 μm [2]. For this reason, numerical modeling such as Finite Element Method (FEM) is an attractive approach to alleviate the required experimental efforts. This technique can predict fundamental variables such as stresses, strains, strain-rates and temperatures, and other relevant variables for industrial applications, i.e. tool-life, residual stresses and burr formation [3].

FEM in chip formation exists since seventies [4] and it has been continuously growing and developing until today. In recent years, with the increasing development of available computational power, FEM has been evolved and extensively used for machining modeling. Significant efforts have been recently focused on improving and applying this method to tool wear modeling and simulation [5,6], temperature prediction in workpiece deformation zones and at the tool tip [7–10] , tool-chip contact behavior simulation [11–13], prediction of residual stress at workpiece surface [14,15] and also microstructure and crystal plasticity analysis during cutting [16–19] .

Despite the broad application of the FEM in modeling and simulation of machining, proper implementation of this technique is still very complex and associated to main problems as, for example, stick-slip behavior of tool and chip at contact area with extreme strain deformation rates ($10^3$-$10^6$ $s^{-1}$). As a consequence of the severe plastic deformation undergone by the material, a strong chance of mesh distortion exists in FE simulation if grid points are fixed to

material points and implementation of separation criteria — as in case of Lagrangian formulation [20] — which causes deterioration of results [21] . To alleviate this drawback, there are three main techniques used in metal cutting FE simulation [22] to avoid mesh distortion and keep the proper mesh quality, such as the automatic Continuous Remeshing of Lagrangian domain (CRL) [23] , the Arbitrary Lagrangian Eulerian (ALE) technique [24] and the pure Eulerian technique [25] . From the analysis of the FE machining simulation literature, it is evident that CRL and ALE approaches are more popular than pure Eulerian technique since this latter has never reached a satisfactory level for machining modeling and simulations. The aim of this study is therefore to develop a Eulerian FE model, suitable for workpiece deformation and chip formation modelling in micro cutting. Micro cutting presents some specific challenging aspects compared to macro cutting in FE modeling. For instance, proper care should be addressed to simulation of material deformation in tool edge region, since localized severe deformations caused by the unavoidable finite cutting edge radius, play a significant role on chip formation process. A proper deformation modeling in this area can lead to a better understanding of process mechanics. Based on this reasoning and on the nature of Lagrangian method, simulation of micro machining cannot be effectively handled with this technique that necessarily requires the implementation of separation criteria [21] where it leads to poor tool edge-chip contact simulations. In fact, previous studies argue that using node separation criteria disturbs material deformation beneath the edge [12,21]. Therefore, the already mentioned CRL [23,19], ALE [26] and Eulerian [27] options remain suitable for micro machining process simulation since they maintain mesh quality on contact while using material plasticity to form a chip and by not requiring any separation criteria. The advantages and drawbacks of these three formulations are well described in [28] and [22]. Despite advantages of ALE and CRL and popularity of these techniques in machining FE simulation literature, there are some drawbacks, such as amount of computational effort, that hold them back. In fact, these two techniques might provide results for 2D simulation with reasonable computational time but the issue of required time for single simulation becomes more evident with 3D models. In fact, with Eulerian approach where the mesh is fixed, it would be possible to reduce the time of each 3D simulation by modifying the size of mesh on critical part of the model, so it is possible to carry out complex 3D cutting processes with reasonable

computational effort where this gives Eulerian technique an advantage over two other techniques.

The biggest shortcoming of the Eulerian technique, basing on [28] and [22], consists in the necessity to have prior knowledge about the chip flow. However, the advantages of this technique — such as low computational effort, no need for separation criteria and possibility to simulate material extreme deformations — still makes it an interesting approach for metal cutting FE analysis.

Simulation modeling with CEL approach exists for many years [29] and has been used in different types of applications, hull explosion under water [30], penetration into soil in geomechanical problems [31–33] , and water jet machining [34,35], but no applications have been found on micro machining process.

Based on this lack, this study presents a Coupled Eulerian Lagrangian (CEL) modelling of micro machining. In the proposed development, the workpiece takes advantages of Eulerian technique while tool is defined as Lagrangian part of the model, then exploring the actual capability of Eulerian technique in micromachining modelling.

In addition, a dedicated experimental campaign is carried out and cutting forces along with chip thickness have been captured and compared to simulated ones to validate the prediction performance of the developed CEL approach. Further investigations on tool tip temperature and contact pressure are offered through the comparison-based analysis of simulation outputs. Eventually, a comparison between actual performance of CEL approach and standard ALE approach is showed to support the reliability of the proposed method.

## 2. Method: CEL model development

In this study, process simulation is performed with the Abaqus/Explicit software package [36] . Full thermo-mechanical process specifications for workpiece, tool and contact are provided as inputs. For workpiece body, Eulerian approach is adopted to simulate the material extreme deformation and chip formation while for tool body Lagrangian technique is used. In the Eulerian description, the material points are independent from mesh grids. CEL approach bases respectively on i) Lagrangian calculation, ii) Eulerian calculation and iii) coupling calculations between these two different domains. With this approach, first pressure is determined from the Eulerian part of the simulation, then this pressure acts on the Lagrangian part of the simulation

through the penalty contact method to couple the Lagrangian and Eulerian parts [27,29,30,32] . The developed 3D CEL model of the micro orthogonal cutting process has the following characteristics:

i) fully thermo-mechanical properties of tool and workpiece are considered
ii) the chip forms along the tool rounded edge directly from the workpiece plastic deformation.
iii) no separation criteria are used for chip formation
iv) one Eulerian domain is introduced to include all together the whole deformation zone taking place in the cutting action and chip formation
v) mesh density is varied within the domain to reach simulation time efficiency and accuracy of tool-chip contact analysis
vi) chip forms automatically from incipient workpiece stage without adjustment of its shape into the process simulation
vii) overall computational is reduced by avoiding frequent remeshing and node displacement

**2.1. Geometric modeling and boundary conditions**

In the assembly of tool and workpiece, Figure 1, the whole Eulerian domain (box *ACDE*) is meshed with an 8-node thermally coupled linear Eulerian (*EC3D8RT*) element type [37] and this mesh distributed uniformly within the domain with size of 50 μm, except the area of possible contact (box *abcd*), where the mesh size is assigned equal to 10 μm.

Tool is meshed with an 8-node thermally coupled (*C3D8T*) element type [37] and this mesh is distributed uniformly with size of 50 μm on the body of this Lagrangian part, with a refinement on the rounded edge (25 μm).

The mesh sizes have been selected by performing preliminary sensitivity analyses on the process outputs. The selected setting resulted the best to accomplish the accuracy and computational time requirements.

The tool is fixed in space by applying displacement boundary conditions (U1=U2=U3=UR1=UR2=UR3=0) (U refers to displacement, UR refers to rotation along the axis and subscripts 1-3 refer to X, Y and Z directions respectively) on both its rear and upper side (I II, II III). Cutting speed, is assigned as initial velocity to the workpiece nodes at the

incipient stage (*ABFG*). In this case the material is also fixed at the lower side to prevent movements along the Y direction. A reference point (RP) is defined in the middle position of the cutting edge radius ($r_e$=60 µm) for extraction of temperature and contact pressure for further investigations.

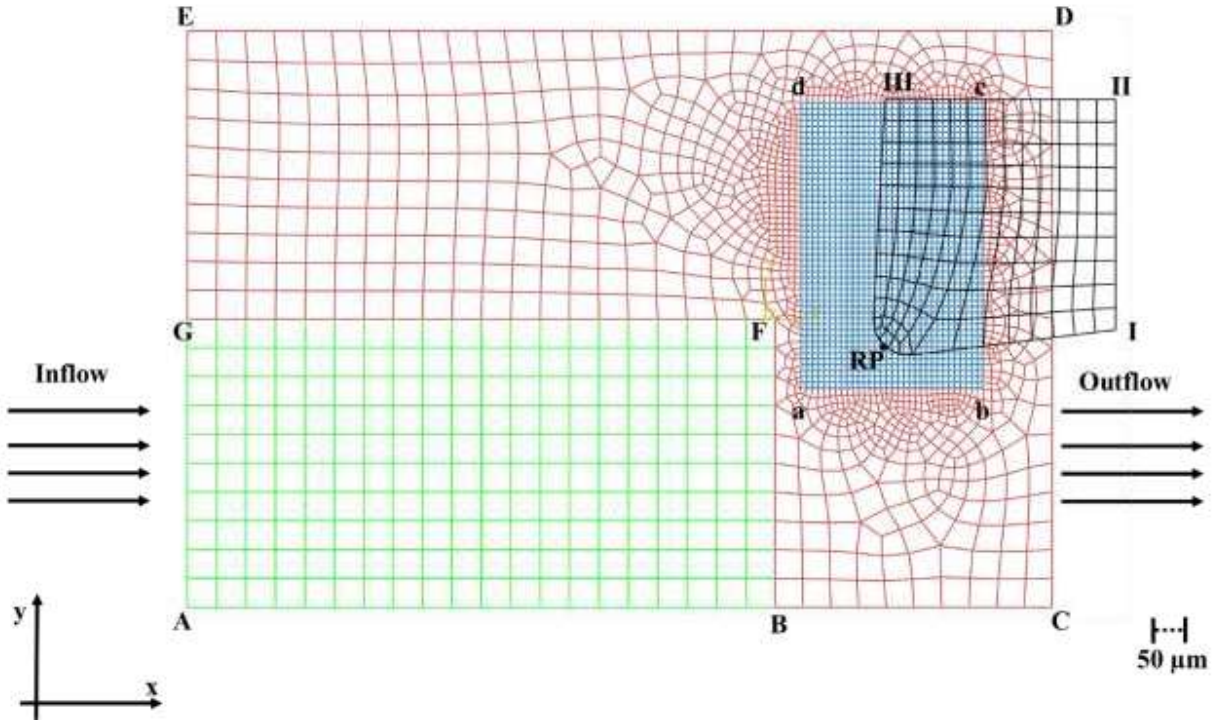


*Figure 1. Tool-workpiece assembly of the CEL approach*

### 2.2. Thermo-mechanical material properties

The study focuses on micro cutting of AISI1045 with uncoated carbide tools, which represents a reference case for many machining research studies [36,38] . Workpiece plastic deformation is modeled with Johnson-Cook flow stress model[39] (Equation 1 and 2) described as follow:

$$\sigma = [A + B(\varepsilon)^n]\left[1 + Cln\left(\frac{\dot{\varepsilon}}{\dot{\varepsilon}_0}\right)\right][1 - T_H^m] \quad (1)$$

$$T_H = \left(\frac{T - T_{room}}{T_{melt} - T_{room}}\right) \quad (2)$$

$\sigma$ is the flow stress, $A$ is the initial yield stress at room temperature, $B$ is the strain hardening coefficient, $C$ is the strain rate sensitivity coefficient, $m$ is the thermal softening exponent, $n$ is

the strain hardening exponent, $\varepsilon$ is the plastic strain, $\dot{\varepsilon}$ is the strain rate, $\dot{\varepsilon}_0$ is the reference strain rate. $T_H$ is the homologous temperature, which is a function of $T$, the absolute temperature, $T_{room}$, the room temperature, and $T_{melt}$, the melting temperature. The Johnson-Cook parameters for the AISI1045 material are taken from [40] , where they were captured through Split Hokinson Pressure Bar (SHPB) tests at high strain rates and temperatures. Thermo-mechanical materials inputs for both uncoated carbide tool and AISI1045 workpiece are reported in Table 1.

### 2.3. Contact modeling

When machining is scaled-down from macro to micro, the importance of the edge geometry increases since uncut chip thickness becomes comparable in size with it and the process mechanics becomes more sensitive to interfacial behavior of cutting edge radius and chip. The high plastic deformation generating high stresses, strains and temperatures, makes the contact behavior modeling more complex. In this study, the following relations (Equation 3 and 4) are adopted for modeling the stick-slip behavior on contact zone [37] :

$$\tau_f < \tau_{crit} \quad \text{Sticking} \tag{3}$$

$$\tau_f = \tau_{crit} \quad \text{Slipping} \tag{4}$$

where $\tau_f$ is the contact shear stress and $\tau_{crit}$ is a critical stress calculated as (Equation 5)

$$\tau_{crit} = \min(\mu p, k_f) \tag{5}$$

where $\mu$ is the Coulomb friction coefficient, $p$ is the contact pressure and $k_f$ is the shear stress threshold for the target material, calculated as $\sigma_y/\sqrt{3}$, being $\sigma_y$ the target material yield stress. Friction modelling is playing big role is standard simulation of machining and there are studies in literature of machining addressing contact behavior during the cutting of AISI1045[41,42]. For fully thermal analysis and heat transfer between tool and chip, the contact heat generation

parameters and thermal contact conductance are also introduced into the model. Table 2 indicates full model inputs for the contact formulation of this study.

*Table 1. Thermo-mechanical properties of AISI 1045 and uncoated carbide tool* [11,40]

| ***Parameters*** | ***Value*** | |
|---|---|---|
| | ***Workpiece*** | ***Tool*** |
| **Thermo-mechanical properties [8]** | ***AISI1045*** | ***Uncoated carbide*** |
| $E$: Elastic modulus | 200 GPa | 8000 GPa |
| $\rho$: Density | 7800 kg/m$^3$ | 15000 kg/m$^3$ |
| $\nu$: Poisson's ratio | 0.3 | 0.2 |
| $c$ : Specific heat | 432.6 J/(kg·°C) | 203 J/(kg·°C) |
| $\alpha_T$: Thermal expansion | 11 µm/(m·°C) | 4.7 µm/(m·°C) |
| $\lambda$: Thermal conductivity | 47.7 W/(m·°C) | 46 W/(m·°C) |
| $\beta_T$ : Inelastic heat fraction | 0.9 | - |
| **Johnson-Cook constants [35]** | | |
| $A$: Initial yield stress at room temperature | 553.1 MPa | - |
| $B$: Strain hardening coefficient | 600.8 MPa | - |
| $C$ : Strain rate sensitivity coefficient | 0.0134 | - |
| $m$ : Thermal softening exponent | 1 | - |
| $n$ : Strain hardening exponent | 0.234 | - |
| **Johnson-Cook inputs** | | |
| $\dot{\varepsilon}_0$ : Reference strain rate [40] | 1 1/s | - |
| $T_{melt}$ : Melting temperature [40] | 1460 °C | - |
| $T_{room}$ : Room temperature | 25 °C | - |

*Table 2. Contact parameters*

| **Contact parameters** | **Value** |
|---|---|
| Coulomb friction coefficient [11] | 0.45 |
| Shear stress threshold [11] | 319.3 MPa |
| Fraction of dissipated energy converted to heat | 1 |
| Fraction of converted heat to master and slave bodies | 0.5 |
| Thermal conductance | $1\times10^8$ (W/m$^2$·°C) |

## 3. Comparison study between CEL and ALE techniques in FE simulation of micro cutting process

Eventually, to evaluate CEL and ALE approaches in FE analysis of micromachining process a case study is implemented. ALE modelling has been already implemented for micro cutting process in previous studies by the authors [26,27] . Differently for those studies, in this case study a 3D ALE model is implemented, to compare the two 3-dimensional approaches. The effort has been made to make these two techniques with as equal as possible inputs. The only difference in modeling setups of these two techniques are in element type and number of nodes included in the model.

*Table 3. Comparison study inputs for CEL and ALE techniques*

| | ***CEL*** | ***ALE*** |
|---|---|---|
| **Simulation inputs** | | |
| Dimension | 3D | 3D |
| Element type | EC3D8R | C3D8R |
| Mesh geometry | 10 µm × 5 µm | 10 µm × 5 µm |
| Number of nodes on workpiece | 11716 | 13122 |
| Type of thermal analysis | Adiabatic | Adiabatic |
| Tool | Rigid | Rigid |
| Distance to engagement | 200 µm | 200 µm |
| Time period | 0.95 ms | 0.95 ms |
| Workpiece material | AISI1045 | AISI1045 |
| Contact formulation | Modified coulomb | Modified coulomb |
| $vc$ (Cutting Speed) | 300 (m/min) | 300 (m/min) |
| $h_c$ (Uncut chip thickness) | 40 µm | 40 µm |

The geometry of mesh stays constant for entire simulation time in CEL and not in ALE. Considering that in CEL the whole deformation area requires to be meshed, the number of nodes on workpiece includes initial workpiece and void. The distance to engagement indicates the initial distance from center of cutting edge radius to workpiece edge (see the Results paragraph for details, Table 5 and Figure 8). Same material and contact characteristics have been setup where applicable for this comparison, following Table 1 and Table 2, respectively.

## 4. Experimental setup for validation

Micro orthogonal cutting tests have been carried out with Sandvik uncoated carbide tool inserts (*DCMT 07 02 04-KM H13A*) (Figure 2d and Table 1) on a ultra-precision Kern EVO 5-axis

machining center (Figure 2b) with nominal positioning accuracy of ± 1 μm, used as a turning machine. Tubular AISI 1045 specimens (Figure 2d) with wall thickness of 0.65 mm have been adopted as workpieces. Focus variation non-contact measuring machine (Alicona Infinite Focus ®) (Figure 2a) has been used for tool topography (Figure 2e) and chip thickness (Figure 2c) measurements. Tool characteristics measured via Alicona microscope, are showed in Table 4.

*Table 4. Geometrical characteristics of the adopted tools*

| Insert Model | Sandvik DCMT 07 02 04-KM H13A |
|---|---|
| Cutting edge radius ($r_e$) | 60 μm |
| Rake angle ($\gamma$) | 3° |
| Clearance angle ($\alpha$) | 7° |

The chip thickness is measured in 5 different positions and the mean value is considered as an output of the experiments. The cutting and thrust forces are captured online with the use of Kistler 9257-BA triaxial load cell (Figure 2d) and the mean value of the force signal during turning operations is considered as the force output magnitude. Two factors have been investigated, namely cutting speed *vc* and uncut chip thickness *hc*, each one varied on two levels (40 μm and 60 μm for *hc* and 100 m/min and 300 m/min for *vc*) and two replicates have been performed, which in total contributes to 8 randomized experiments. The *hc* are chosen to be comparable to the edge radius to reflect usual conditions happening in micro scale cutting.

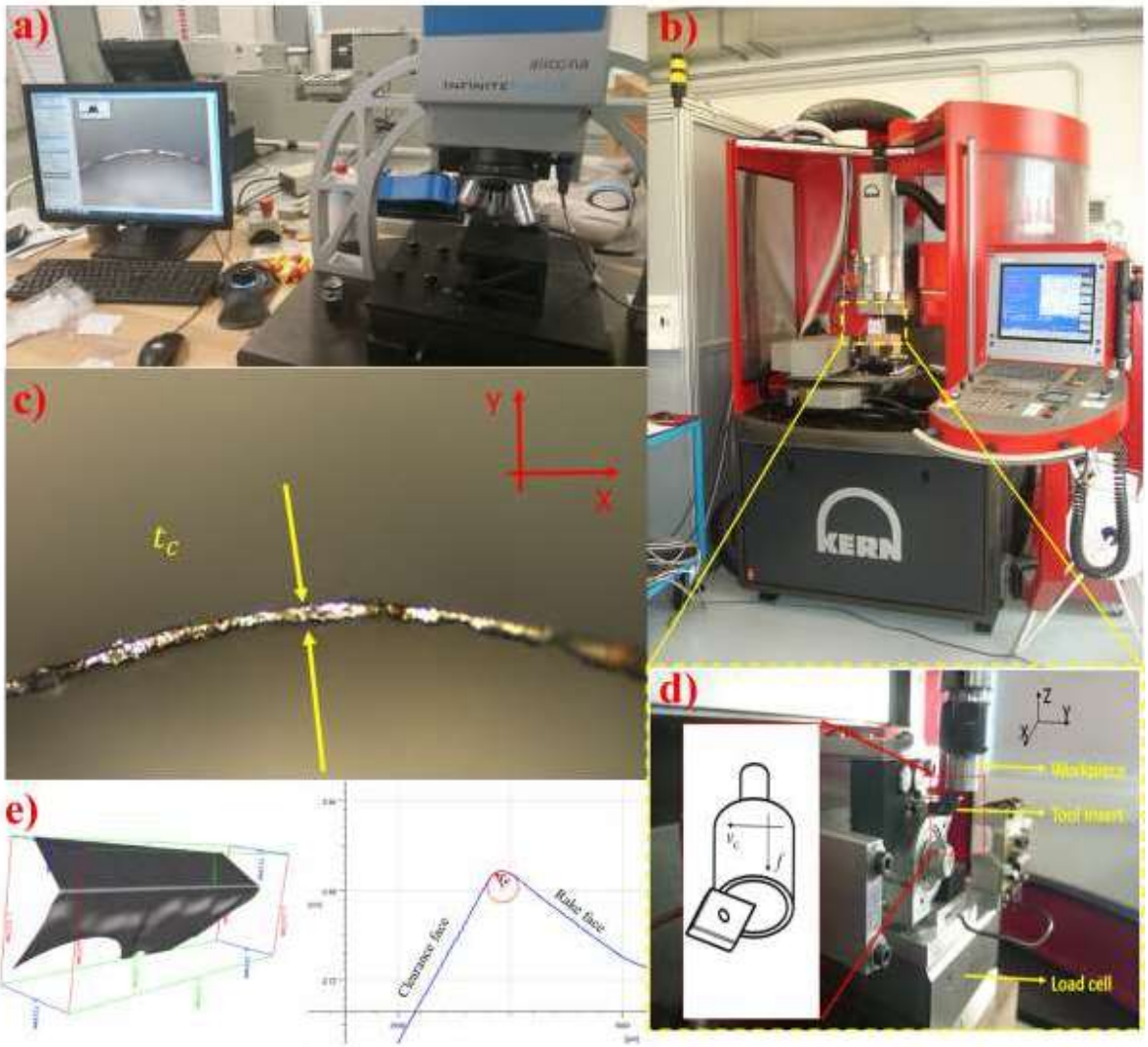


*Figure 2. Experimental setup and description of the micro orthogonal cutting*

## 5. Results and discussion

### 5.1. CEL modelling Results

#### 5.1.1. Chip Thickness and Forces

The extracted experimental quantities (chip thickness, cutting and thrust forces) are compared with predicted ones and prediction performances are quantified basing on *Mean Percentage Error* of the prediction in respect to the experimental values, Figure 3. Figure 3 indicates the error for all cutting conditions and outputs, while Figure 4 illustrates the final step of chip formation with the CEL approach. As stated in the modeling section of this work, with this

approach it is possible to achieve the final chip geometry from the workpiece incipient stage and, this way, the improvement is achieved compared to the previous pure Eulerian technique [26] , where the simulations were carried out with the introduction of the initial chip flow zone. Figure 4 clearly indicates the "Curling back" effect in micromachining with different parameters. Figure 4 illustrates that, when the uncut chip thickness changes from being equal to edge radius of the tool to lower than that, then chip starts to curl back more intensively. Furthermore, cutting speed is also playing role on "Curling back", for instance, lower cutting speed provides the opportunity for the chip to stay closer to the rake face of the tool while higher cutting speed pushes the chips away from contact zone. Mean error changes for each output but always keeps under 20%. Error on cutting force (Figure 3a) with $hc$ = 60 µm, equal to edge radius and with both $vc$ values, shows lower values compared to the lower $hc$ (7% and 15%, respectively). In case of the thrust force, the error varies from case to case and the best estimated thrust force (10.8% of mean error) is for the cutting condition with $vc$ = 100 m/min and $hc$ = 60 µm. The mean errors on the chip thickness are the smallest ones since all of them are below 6%. The range of 20% error between simulation and experiments could be reasonable in micro scale cutting, as claimed by [7] , so the potential of the CEL approach in the FE modeling of the micro cutting process is approved by the presented results.

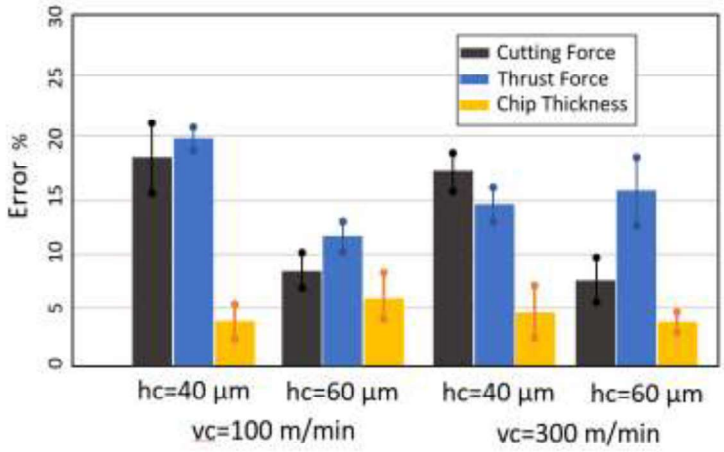


*Figure 3. Mean Percentage Error (MPE) for the prediction of Cutting force, Thrust force, Chip thickness*

### 5.1.2. Temperature and contact pressure

Tool tip temperature and the contact pressure are fundamental variables for studying tool-chip contact condition during cutting action but with the state of the art sensing technologies they are extremely difficult to capture from experiments in micro scale cutting processes. These quantities are extracted from simulation at the reference point introduced in Figure 1 (point RP) at the final simulation step (Figure 5 and Figure 6). Main effects plots, Figure 7, enable the analysis of differences between level means for each single factor without considering mutual interactions [43]. Figure 7a confirms that tool tip temperature is sensitive to cutting speed: by increasing *vc* from 100 m/min to 300 m/min, the tool tip temperature increases from 487 °C to 685 °C. On the other hand, the increase of *hc* does not significantly increase the tool tip temperature (passing from 582 °C to 590 °C). This fact reveals that in cutting actions with *hc* comparable to the edge radius, heat generation is not significantly affected by this factor, but it is sensitive with changes of *vc*.

Contact pressure on the tool tip also increases (from 1495 MPa to 1615 MPa) when *vc* increases from 100 m/min to 300 m/min, Figure 7b. Moreover, *hc* is playing a minor role on the contact pressure variation at the tool tip. In fact, the contact pressure slightly increases (from 1525 MPa to 1585 MPa) by increasing *hc* from 40 µm to 60 µm, Figure 7b. Figure 7a and 7b show that higher cutting speed increases both contact pressure and temperature at the tool tip when cutting with uncut chip thickness comparable or lower that edge radius of the tool. Contact pressure is a function of forces on the contact zone to area of tool-chip contact, as indicated also in figure 4, because of higher chip curl back with higher cutting speed the area of contact decreases so the pressure is higher and because of frictional behavior the shear stress and temperature on tool are higher.

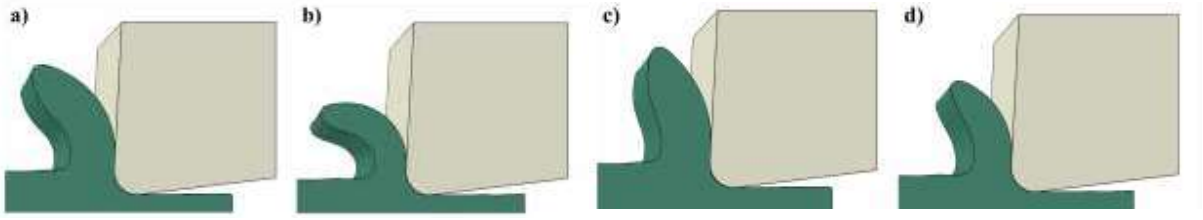


*Figure 4. Chip formation with CEL approach, a) vc = 300 m/min, hc = 60 µm, b) hc 300 m/min, hc = 40 µm, c) $v_C$ = 100 m/min, hc = 60 µm, d) $v_C$ = 100 m/min, hc = 40 µm*

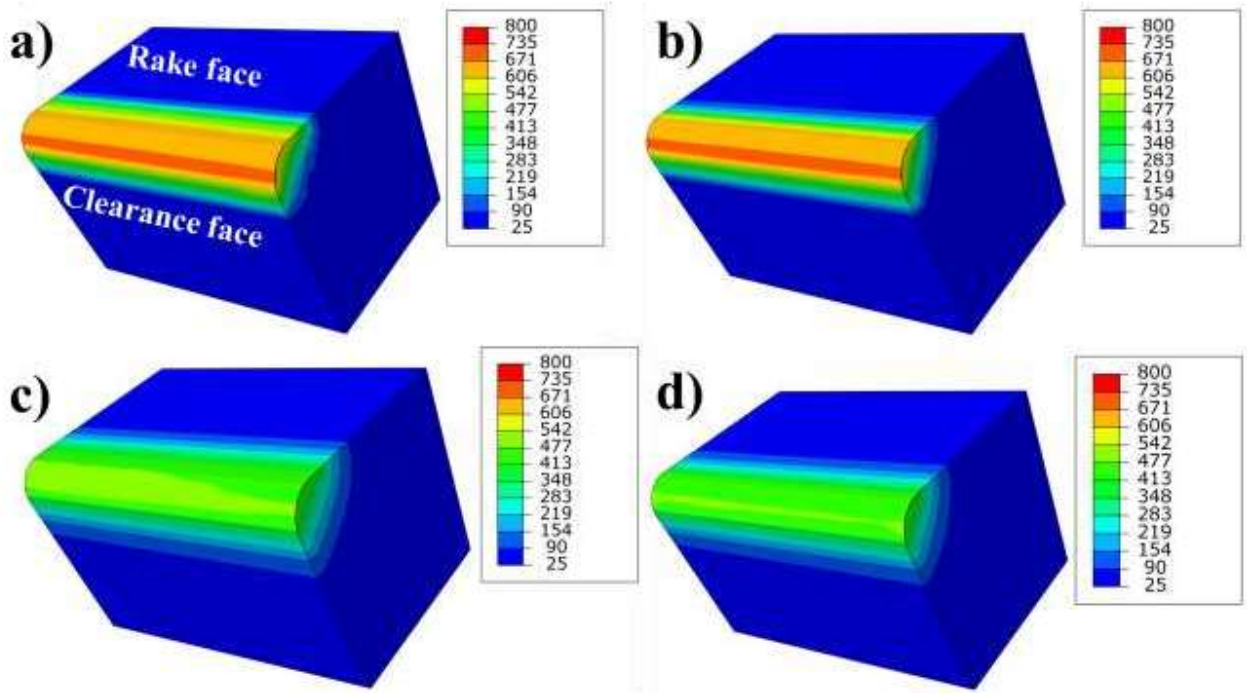


*Figure 5. Tool tip temperature (°C), a) vc=300 m/min, hc=60 µm, b) vc=300 m/min, hc=40 µm, c) vc=100 m/min, hc=60 µm, d) vc=100 m/min, hc=40 µm*

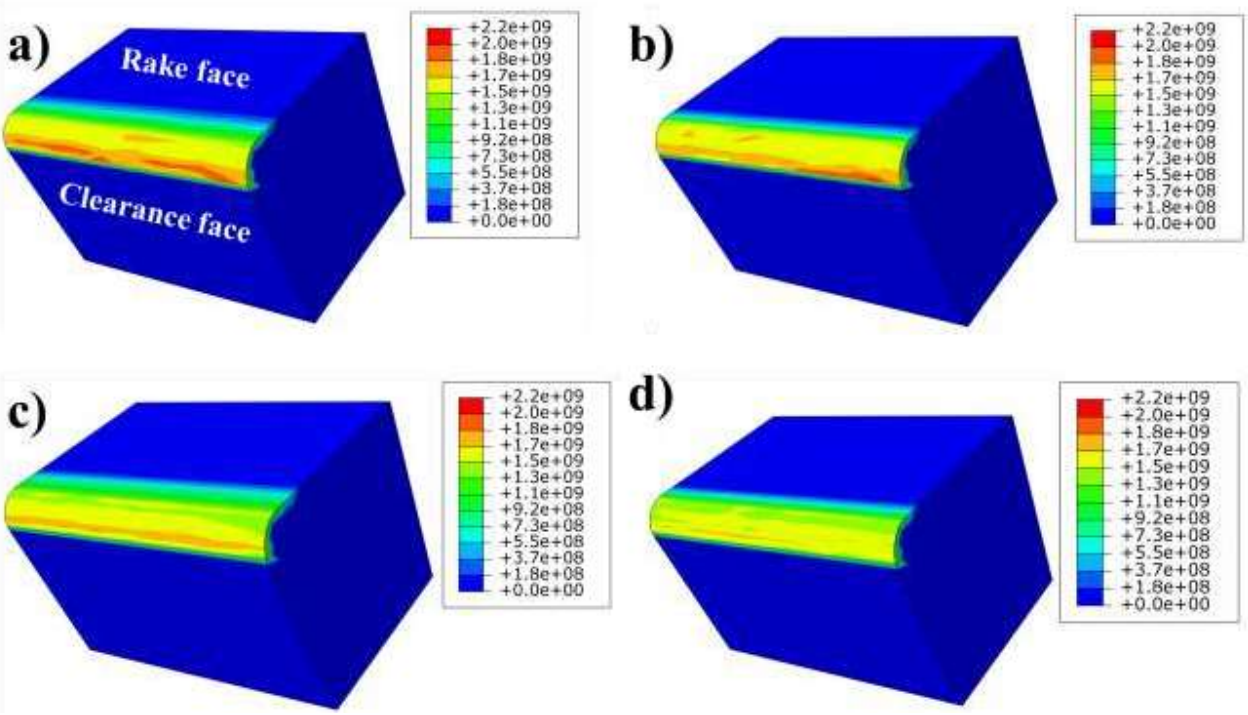


*Figure 6. Contact pressure (Pa), a) vc=300 m/min, hc=60 µm, b) $v_C$=300 m/min, hc=40 µm, c) vc=100 m/min, hc=60 µm, d) $v_C$=100 m/min, hc=40 µm*

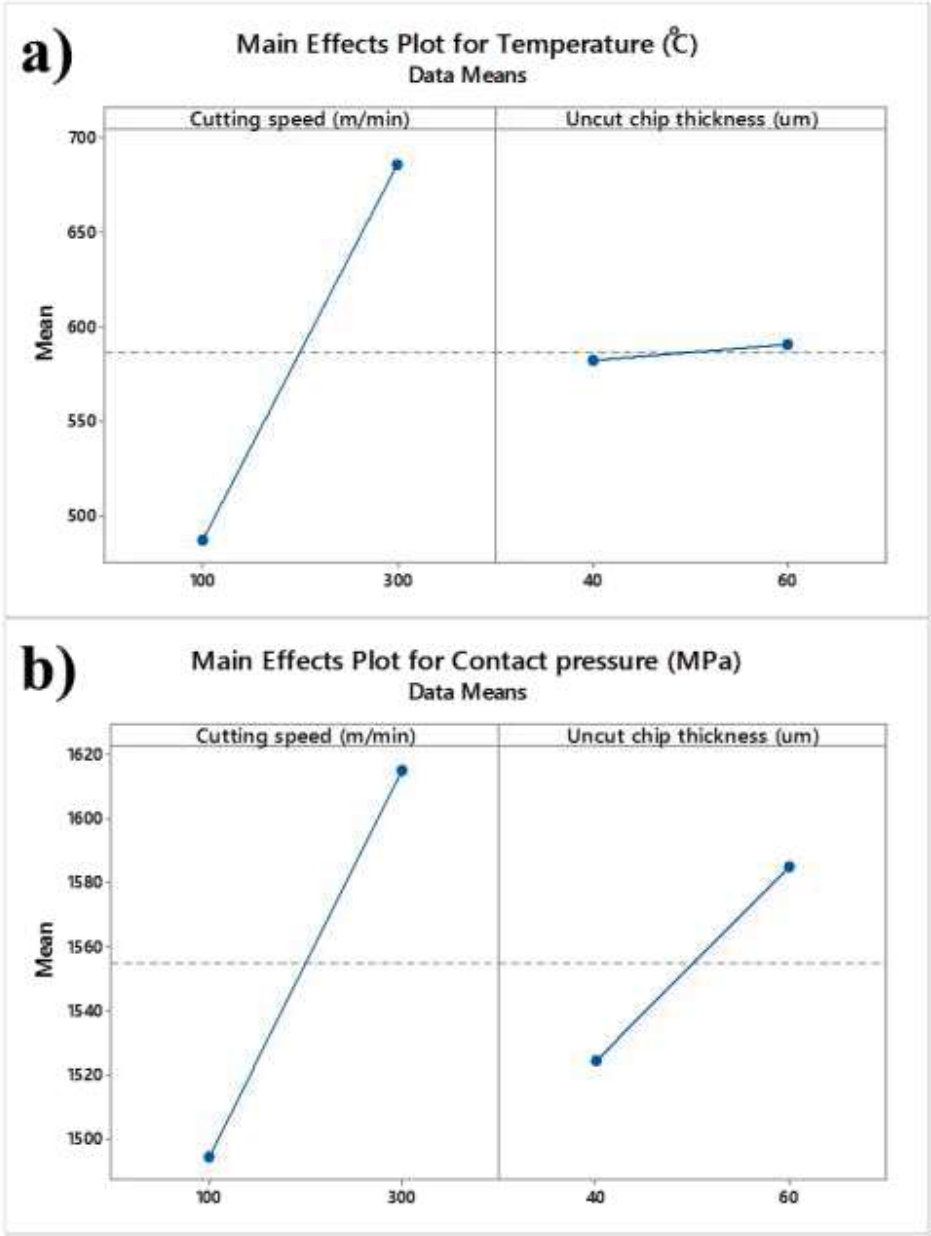


*Figure 7. Main effects plot a) Tool tip temperature, b) Contact pressure at reference point*

### 5.2. Comparison between CEL and ALE

The summary and results of two models are reported in Table 3 and chip formation for each is illustrated in Figure 8. The comparison between CEL and traditional ALE approach gave interesting results. Simulation outputs indicate that CEL is more expensive in terms of computational time (simulations are executed with single processor on Intel(R) Core(TM) i7-4500U CPU @ 1.80GHz) while this technique showed a better prediction performance for all of process outputs. In conclusion of this case study, CEL model despite of its demand for more computational power can predict simulation outputs better than ALE approach.

*Table 5. Thermo-mechanical properties of AISI 1045 and uncoated carbide tool [9,36]*

| | ***CEL*** | ***ALE*** |
|---|---|---|
| **Simulation outputs** | | |
| Computational time | 95 Min and 12 Sec | 79 Min and 47 Sec |
| MPE Cutting Force | 22.8 % | 31.1 % |
| MPE Thrust Force | 19.0 % | 35.2 % |
| MPE Chip thickness | 7.43 % | 10.6 % |

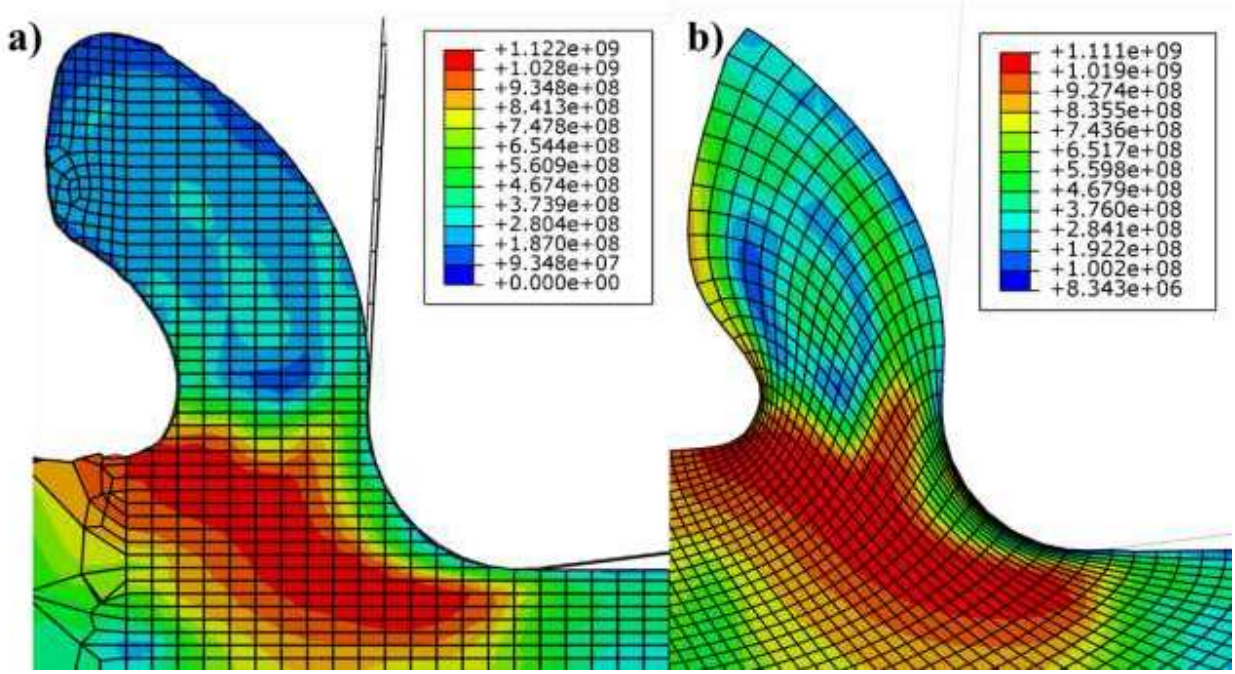


*Figure 8. Von Mises stress (Pa) distribution in FE simulation of microcutting a) CEL model, b) ALE model*

## 6. Conclusion

CEL approach can be an attractive technique for FE modeling of metal cutting since the topography of the mesh (shape and size) is constant during the simulation and material flows within the domain and independent of mesh. Therefore, there are two advantages behind this modeling technique: i) the mesh cannot be distorted, ii) the computational effort can be adjusted by localized mesh refinement. Eventually, these two factors are very important in every machining simulations. This study explored the capability of CEL approach in predicting micro cutting process outputs by considering fully thermo-mechanical input parameters of working materials and contact properties. A 3D model has been built and experiments have been carried out to validate the achieved performance. Results indicate that there is a good potential for the use of the CEL approach in the material removal process simulation at the micro scale. This study revealed that the developed CEL model predicts the micro scale cutting process outputs with reasonable accuracy, i.e. with mean errors less than 20%.

Further investigations have been dedicated to study the effects of uncut chip thickness and cutting speed changes on tool tip temperature and contact pressure. According to the simulation results, the following remarks can be summarized in micro cutting conditions where uncut chip thickness is lower than the cutting edge radius:

1. The tool tip temperature increases with cutting speed and uncut chip thickness and the amount of this increase is more pronounced with the cutting speed growth.
2. The contact pressure at the tool tip is also subjected to the same behavior as the tool tip temperature when cutting speed increases. In fact, simulation outputs illustrate that the contact pressure is higher for high cutting speeds compared to low cutting speeds.

## References

[1] D. Dornfeld, D.-E. Lee, eds., Precision machining processes BT - Precision Manufacturing, in: Springer US, Boston, MA, 2008: pp. 455–554. doi:10.1007/978-0-387-68208-2_10.

[2] T. Masuzawa, H.K. Tönshoff, Three-Dimensional Micromachining by Machine Tools,

CIRP Ann. - Manuf. Technol. 46 (1997) 621–628. doi:10.1016/S0007-8506(07)60882-8.

[3] P.J. Arrazola, T. Özel, D. Umbrello, M. Davies, I.S. Jawahir, Recent advances in modelling of metal machining processes, CIRP Ann. - Manuf. Technol. 62 (2013) 695–718. doi:10.1016/j.cirp.2013.05.006.

[4] Y. Kakino, Analysis of the mechanism of orthogonal machining by the finite element methode, J, Japan Soc. Prec. Eng. 37 (1971) 503–508.

[5] A. Muñoz-Sánchez, J.A. Canteli, J.L. Cantero, M.H. Miguélez, Numerical analysis of the tool wear effect in the machining induced residual stresses, Simul. Model. Pract. Theory. 19 (2011) 872–886. doi:10.1016/j.simpat.2010.11.011.

[6] A. Attanasio, D. Umbrello, C. Cappellini, G. Rotella, R. M'Saoubi, Tool wear effects on white and dark layer formation in hard turning of AISI 52100 steel, Wear. 286–287 (2012) 98–107. doi:10.1016/j.wear.2011.07.001.

[7] G. Chen, C. Ren, P. Zhang, K. Cui, Y. Li, Measurement and finite element simulation of micro-cutting temperatures of tool tip and workpiece, Int. J. Mach. Tools Manuf. 75 (2013) 16–26. doi:10.1016/j.ijmachtools.2013.08.005.

[8] T. Thepsonthi, T. Özel, 3-D finite element process simulation of micro-end milling Ti-6Al-4V titanium alloy: Experimental validations on chip flow and tool wear, J. Mater. Process. Technol. 221 (2015) 128–145. doi:10.1016/j.jmatprotec.2015.02.019.

[9] Y. Karpat, T. Ozel, Process simulations for 3D turning using uniform and variable microgeometry PCBN tools, Int. J. Mach. Mach. Mater. 4 (2008) 26. doi:10.1504/IJMMM.2008.020908.

[10] C. Maranhao, J.P. Davim, M.J. Jackson, G. Cabral, J Gracio, FEM machining analysis: influence of rake angle in cutting of aluminium alloys using Polycrystalline Diamond cutting tools, Int. J. Mater. Prod. Technol. 37 (2009) 199–213. doi:10.1504/IJMPT.2010.029469.

[11] K.S. Woon, M. Rahman, K.S. Neo, K. Liu, The effect of tool edge radius on the contact phenomenon of tool-based micromachining, Int. J. Mach. Tools Manuf. 48 (2008) 1395–1407. doi:10.1016/j.ijmachtools.2008.05.001.

[12] P.J. Arrazola, T. Özel, Investigations on the effects of friction modeling in finite element simulation of machining, Int. J. Mech. Sci. 52 (2010) 31–42. doi:10.1016/j.ijmecsci.2009.10.001.

[13] W. Grzesik, P. Nieslony, Coupled thermo-mechanical FEM-based modelling of the tool-chip contact behaviour for coated cutting tools, Int. J. Mach. Mach. Mater. 11 (2012) 20. doi:10.1504/IJMMM.2012.044920.

[14] M.N.A. Nasr, E.-G. Ng, M.A. Elbestawi, A modified time-efficient FE approach for predicting machining-induced residual stresses, Finite Elem. Anal. Des. 44 (2008) 149–161. doi:10.1016/j.finel.2007.11.005.

[15] M. Mohammadpour, M.R. Razfar, R. Jalili Saffar, Numerical investigating the effect of machining parameters on residual stresses in orthogonal cutting, Simul. Model. Pract. Theory. 18 (2010) 378–389. doi:10.1016/j.simpat.2009.12.004.

[16] G. Ljustina, R. Larsson, M. Fagerström, A FE based machining simulation methodology accounting for cast iron microstructure, Finite Elem. Anal. Des. 80 (2014) 1–10. doi:10.1016/j.finel.2013.10.006.

[17] M. Abouridouane, F. Klocke, D. Lung, O. Adams, A new 3D multiphase FE model for micro cutting ferritic–pearlitic carbon steels, CIRP Ann. - Manuf. Technol. 61 (2012) 71–74. doi:10.1016/j.cirp.2012.03.075.

[18] S.A. Tajalli, M.R. Movahhedy, J. Akbari, Simulation of orthogonal micro-cutting of FCC materials based on rate-dependent crystal plasticity finite element model, Comput. Mater. Sci. 86 (2014) 79–87. doi:10.1016/j.commatsci.2014.01.016.

[19] J.P. Davim, P. Reis, C. Maranhao, M.J. Jackson, G. Cabral, J. Gracio, Finite element simulation and experimental analysis of orthogonal cutting of an aluminium alloy using Polycrystalline Diamond tools, Int. J. Mater. Prod. Technol. 37 (2010) 46. doi:10.1504/IJMPT.2010.029458.

[20] M. Movahhedy, M.S. Gadala, Y. Altintas, Simulation of the orthogonal metal cutting process using an arbitrary Lagrangian–Eulerian finite-element method, J. Mater. Process. Technol. 103 (2000) 267–275. doi:10.1016/S0924-0136(00)00480-5.

[21] M.R. Movahhedy, ALE Simulation of chip formation in orthogonal metal cutting process, PhD thesis, University of British Columbia, 2000.

[22] J.C. Outeiro, D. Umbrello, R. M'Saoubi, I. Jawahir, Evaluation of Present Numerical Models for Predicting Metal Cutting Performance And Residual Stresses, Mach. Sci. Technol. 19 (2015) 183–216.

[23] T.D. Marusich, M. Ortiz, Modelling and simulation of high-speed machining, Int. J. Numer. Methods Eng. 38 (1995) 3675–3694. doi:10.1002/nme.1620382108.

[24] R. Rakotomalala, P. Joyot, M. Touratier, Arbitrary Lagrangian-Eulerian thermomechanical finite-element model of material cutting, Commun. Numer. Methods Eng. 9 (1993) 975–987. doi:10.1002/cnm.1640091205.

[25] J.-D. Kim, V.R. Marinov, D.-S. Kim, Built-up edge analysis of orthogonal cutting by the visco-plastic finite-element method, J. Mater. Process. Technol. 71 (1997) 367–372. doi:10.1016/S0924-0136(97)00099-X.

[26] [Exluded because of journal policy]

[27] [Exluded because of journal policy]

[28] N. Ben Moussa, H. Sidhom, C. Braham, Numerical and experimental analysis of residual stress and plastic strain distributions in machined stainless steel, Int. J. Mech. Sci. 64 (2012) 82–93. doi:10.1016/j.ijmecsci.2012.07.011.

[29] W.F. Noh, CEL: A time-dependent, two-space-dimensional, coupled Eulerian-Lagrange code, Lawrence Radiation Lab., Univ. of California, Livermore, 1963.

[30] D.J. Benson, Computational methods in Lagrangian and Eulerian hydrocodes, Comput. Methods Appl. Mech. Eng. 99 (1992) 235–394. doi:10.1016/0045-7825(92)90042-I.

[31] T. Hamann, G. Qiu, J. Grabe, Application of a Coupled Eulerian–Lagrangian approach on pile installation problems under partially drained conditions, Comput. Geotech. 63 (2015) 279–290. doi:10.1016/j.compgeo.2014.10.006.

[32] K.H. Brown, S.P. Burns, M.A. Christon, Coupled Eulerian-Lagrangian methods for earth penetrating weapon applications, Sand Rep. (2002).

[33] G. Qiu, S. Henke, J. Grabe, Application of a Coupled Eulerian–Lagrangian approach on geomechanical problems involving large deformations, Comput. Geotech. 38 (2011) 30–39. doi:10.1016/j.compgeo.2010.09.002.

[34] Y. Ayed, C. Robert, G. Germain, A. Ammar, Development of a numerical model for the understanding of the chip formation in high-pressure water-jet assisted machining, Finite Elem. Anal. Des. 108 (2016) 1–8. doi:10.1016/j.finel.2015.09.003.

[35] C.-Y. Hsu, C.-C. Liang, T.-L. Teng, A.-T. Nguyen, A numerical study on high-speed water jet impact, Ocean Eng. 72 (2013) 98–106. doi:10.1016/j.oceaneng.2013.06.012.

[36] H. Weule, V. Hüntrup, H. Tritschler, Micro-Cutting of Steel to Meet New Requirements in Miniaturization, CIRP Ann. - Manuf. Technol. 50 (2001) 61–64. doi:10.1016/S0007-8506(07)62071-X.

[37] D. Systèmes, Abaqus analysis user's manual, Simulia Corp. Provid. RI, USA. (2007).

[38] M. Takács, B. Verö, I. Mészáros, Micromilling of metallic materials, J. Mater. Process. Technol. 138 (2003) 152–155. doi:10.1016/S0924-0136(03)00064-5.

[39] W.H.C. G.J. Johnson, A constitutive model and data for metals subjected to large strains, high strain rates and high temperatures, Proc. 7th Int. Symp. Ballist. (1983) 541–547.

[40] S.P.F.. Jaspers, J.. Dautzenberg, Material behaviour in conditions similar to metal cutting: flow stress in the primary shear zone, J. Mater. Process. Technol. 122 (2002) 322–330. doi:10.1016/S0924-0136(01)01228-6.

[41] S.A. Iqbal, P.T. Mativenga, M.A. Sheikh, Contact length prediction: mathematical models and effect of friction schemes on FEM simulation for conventional to HSM of AISI 1045 steel, Int. J. Mach. Mach. Mater. 3 (2008) 18. doi:10.1504/IJMMM.2008.017622.

[42] C. Bonnet, J. Rech, H. Hamdi, E. D'Eramo, Improvement of the numerical modelling in orthogonal dry cutting of an AISI1045 steel by the introduction of a new friction model, Int. J. Mach. Mach. Mater. 9 (2011) 316. doi:10.1504/IJMMM.2011.039654.

[43] D.C. Montgomery, Design and analysis of experiments, John Wiley & Sons, 2008.